Research Article

Journal of CHEMOMETRICS

Received: 8 May 2009, Revised: 11 February 2010, Accepted: 14 February 2010, Published online in Wiley InterScience: 24 May 2010

(www.interscience.wiley.com) DOI: 10.1002/cem.1308

# Non-parametric permutation test for the discrimination of float glass samples based on LIBS spectra

**Erin McIntee[a], Emilie Viglino[a], Stephanie Kumor[a], Caitlin Rinke[a], Liqiang Ni[b]* and Michael E. Sigman[a]***

**Laser-induced breakdown spectroscopy (LIBS) coupled with non-parametric permutation based hypothesis testing is demonstrated to have good performance in discriminating float glass samples. This type of pairwise sample comparison is important in manufacturing process quality control, forensic science and other applications where determination of a match probability between two samples is required. Analysis of the pairwise comparisons between multiple LIBS spectra from a single glass sample shows that some assumptions required by parametric methods may not hold in practice, motivating the adoption of a non-parametric permutation test. Without rigid distributional assumptions, the permutation test exhibits excellent discriminating power while holding the actual size of Type I error at the nominal level. Copyright © 2010 John Wiley & Sons, Ltd.**

**Keywords:** non-parametric permutation test; laser-induced breakdown spectroscopy (LIBS); glass analysis

## 1. INTRODUCTION

Laser-induced breakdown spectroscopy (LIBS) is an analytical technique that aids in the determination of a sample's elemental composition by laser ablation with subsequent recording of the atomic, ionic and molecular emissions from the excited species formed in the laser-induced plasma. Attractive analytical characteristics of LIBS include lack of required sample preparation, rapid analysis and potential field portability. Several reviews of recent developments in the field of LIBS research address the multitude of applications for which this spectroscopic technique has been used [1–4]. Despite its many advantages, LIBS applications have been hindered by limitations that may be partially minimized, including high background continuum, line-broadening and self-absorption [2]. The precision of LIBS data resulting from shot-to-shot laser fluctuations (typically 1–5%) can lead to experimental variations in atomic emission intensities [5]. An average of $6.5 \pm 1.4$ %RSD (relative standard deviation) was reported for a set of 11 emission intensity ratios collected in a single day from averaged LIBS spectra of an NIST SR-610 glass sample [6]. However, the %RSD increased to $24.5 \pm 29.2$% for spectra collected over a 3-day period. The large observed day-to-day variations represent a significant incentive for limiting comparisons to spectra collected on the same day and the use of appropriate statistical testing for sample discrimination.

The precision of LIBS spectra could be an important issue for the potential use of this technique for establishing a database of profiles. However, it is less of a problem for sample classification and discrimination in manufacturing or forensic practice when the samples to be compared are present for testing at the same time and the same location. The samples examined in this work are all float glass taken from automobile side windows. Float glasses are prepared by floating fully homogenized molten glass on a bed of molten tin in a float chamber, which is held at a high temperature [7]. Tin is present on the float side of the glass, extending a very small distance into the sample. The resulting material is of a relatively homogeneous chemical composition on the non-float side. However, a recent study [8] found substantial variation of elemental concentration within float glass panes, which means the spatial information of the samples should be incorporated into comparative analyses. Our experience using LIBS echoes this finding that the source location of the sample on the window could be crucial for discrimination. In this paper, we focus on the violation of distributional assumptions and propose a non-parametric remedy. To avoid inadvertent intra-window variation, all glass samples collected in our experiment are from the center of the automobile side window.

Previous studies have examined the use of LIBS for the discrimination of glass samples through a comparison of elemental emission ratios by parametric multivariate statistical approaches, [6,9] and Student *t*-tests [10]. Discrimination of 83% of the pairwise comparisons of a series of 23 float glass samples was possible at a 99% confidence level ($\alpha = 0.01$) based on LIBS emission intensity ratios employing MANOVA with a Tukey *post hoc* test to analyze the float side of the sample [9]. A 74% discrimination at a 95% confidence level ($\alpha = 0.05$) was reported for the analysis of a series of 27 float glass samples analyzed by LIBS on the non-float side using similar data analysis methods, with higher discrimination found for automobile headlamp (98%) and brown drinking glass

* *Correspondence to: M. E. Sigman, Department of Chemistry and National Center for Forensic Science, University of Central Florida, Orlando, FL 32816, USA.*
*E-mail: lni@mail.ucf.edu; E-mail: msigman@mail.ucf.edu*

a *E. McIntee, E. Viglino, S. Kumor, C. Rinke, M. E. Sigman*
*Department of Chemistry and National Center for Forensic Science, University of Central Florida, Orlando, FL 32816, USA*

b *L. Ni*
*Department of Statistics and Actuarial Sciences, University of Central Florida, Orlando, FL 32816,USA*

(99%) samples and lower discrimination found for automobile side-mirror glass (56%) [6]. Student *t*-test analysis of set of 41 automotive glasses by LIBS has also been reported to result in greater than 99% discrimination, which was nearly identical with micro X-ray fluorescence and laser ablation inductively coupled plasma mass spectrometry (LA-ICP-MS) [10]. A later investigation of the use of linear and rank correlation of LIBS spectra that had been masked to remove some of the more intense lines reported a 100% correct identification of pairwise comparisons of 10 automotive glasses using linear correlation at a 5% significance level [11]. Rank correlation of the masked data was found to give a 93% correct identification at a 5% significance level.

While the results are quite encouraging, these tests rely on the validity of the distributional assumptions. Deviation from these assumptions could render a substantial difference between the actual significance level and the nominal level. In a series of three papers, Curran *et al*. [12–14] have addressed the analysis of glass samples using multi-element composition by Hotelling's $T^2$ test for the comparison of two datasets of multivariate means and eventually the group moved to permutation tests to relieve the distributional assumptions. The intensity of LIBS emissions collected by analog accumulation using both Echelle and Czerny–Turner spectrometers has recently been shown to be derived from a Fréchet extreme value distribution, rather than a normal distribution, a factor that also favors adopting a non-parametric hypothesis testing approach [15].

In this paper, the use of LIBS is examined in combination with a non-parametric permutation approach [16], which is not dependent upon a normal distribution of the comparative figure of merit for the discrimination of automotive glass samples. The analyses given here emphasize the comparison of LIBS spectral data collected from 200 to 900 nm, rather than selected peak ratios or masked spectra. While LIBS data are used in this study, the non-parametric permutation approach is broadly applicable to comparisons of other data types.

In addition to hypothesis testing adopted in this paper, there are many other justifiable approaches to tackle similar tasks. In particular, classification and discrimination of glass fragments' samples for forensic purposes using refractive index and elemental composition coupled with likelihood ratio and Bayesian networks has been studied [17,18]. An overview of classification methods applied to glass analysis using naïve Bayes classifiers and support vector machines can be found in Zadora [19]. For a general background about statistics in forensic science, interested readers may refer to Lucy [20] for details.

## 2. EXPERIMENTAL

### 2.1. Data collection

The LIBS instrument used in this research was an Ocean Optics (Dunedin, Fl, USA), model LIBS2000+ equipped with a Q-switched Nd-YAG laser (9 ns pulse width, Big Sky Lasers, model CFR200, Bozeman, Montana, USA). The plasma was generated by focusing the 1064 nm output from the laser, 65 mJ/pulse (irradiance = 6.6 MW/cm$^2$) and emission intensities (200–900 nm) were collected by a bifurcated fiber optic bundle following an optimized 5 μs detector delay and focused onto an array of seven CCD spectrometers. Spectra were collected under an air atmosphere at ambient pressure and temperature. Data acquisition was performed using the Ocean Optics OOILIBS software. The collection of the spectra was optimized by observation of the intensities of several single shot spectra taken on the surface of a sample as the height of the focusing lens was adjusted. The height of the lens at which the intensity was at its maximum was maintained for all samples since differences between the thicknesses of the samples were minimal. All statistical calculations on the spectra collected in this study were done in R, an open source statistical computing platform [21].

The glass samples used in this research were collected from junk yards in Florida. While there is no guarantee that the glasses did not come from after-market manufacturers, all samples did come directly from different vehicles. The composition of float glasses is known to be altered at their surface by corrosion [22,23]. All samples were cleaned prior to data collection by performing a surface wipe with a KimWipe (Kimberly-Clark Inc. Mississauga, Ontario, Canada) wetted with de-ionized water.

First we consider an initial set of three windows, each from one of the three vehicles: 2000 Volvo S40, 1992 Honda Accord and 2000 Acura Integra, respectively. We cut one large piece from the center of each window. For each piece, we collected 18 spectra, each is an average of 10 single ablation spectra collected at different locations on the sample. All these 54 spectra were collected in completely randomized order within hours. Through this initial study, we gain the knowledge about the magnitude of intra-sample and inter-sample variations expressed in appropriate similarity measures. In the second part of the experiment, we expand our study to 10 different cars. The sample protocol is the same except that there are six spectra for each window. Spectra were all taken on the non-float side of the glass, as determined by visualization under irradiation with 254 nm light (low pressure Hg) [24].

## 3. RESULTS

The main premise is that glasses can be characterized by their spectral profiles which can be stipulated as smooth curves and are determined by the elemental composition. Figure 1 shows one spectrum from each of the initial set, where the log intensities have been normalized from 0 to 1. The actual spectra obtained as shown in Figure 1 are discrete realizations of the profiles. It is easy to see that the spectra are very similar. To examine the relative magnitude of the intra-sample and inter-sample variations, we plot the spectra of the 2000 Volvo shown in Figure 1, against another 2000 Volvo spectrum in Figure 2a, against a 1992 Honda spectrum in Figure 2b and against a 2000 Acura spectrum in Figure 2c, respectively. In each panel, the difference between two spectra is plotted on the vertical axis against the Volvo spectra on the horizontal axis. The inter-sample variations in Figure 2b, c are conspicuously larger than the intra-sample variation in Figure 2a, which serves as the basis for classification.

Suppose we have two sets of samples. We are interested in whether their profiles match each other. In the context of hypothesis testing, the null hypothesis $H_0$ is that their spectral profiles are the same; in other words, we say that they match. The alternative $H_A$ is that there is a mismatch. We regard it as self-evident that the spectral profiles from samples having the same elemental composition should be more similar than those from samples with different elemental compositions. Therefore, appropriate measures of similarity can serve as the basis for discrimination. To help demonstrate the idea, we revisit the initial set of spectra. We use the Fisher transformation of the Pearson correlation coefficient as the similarity score, which will be defined shortly. We examine (a) the 153 similarity scores among the Volvo spectra, (b) the 324 scores between the Volvo and the Honda, (c) the 153 similarity scores

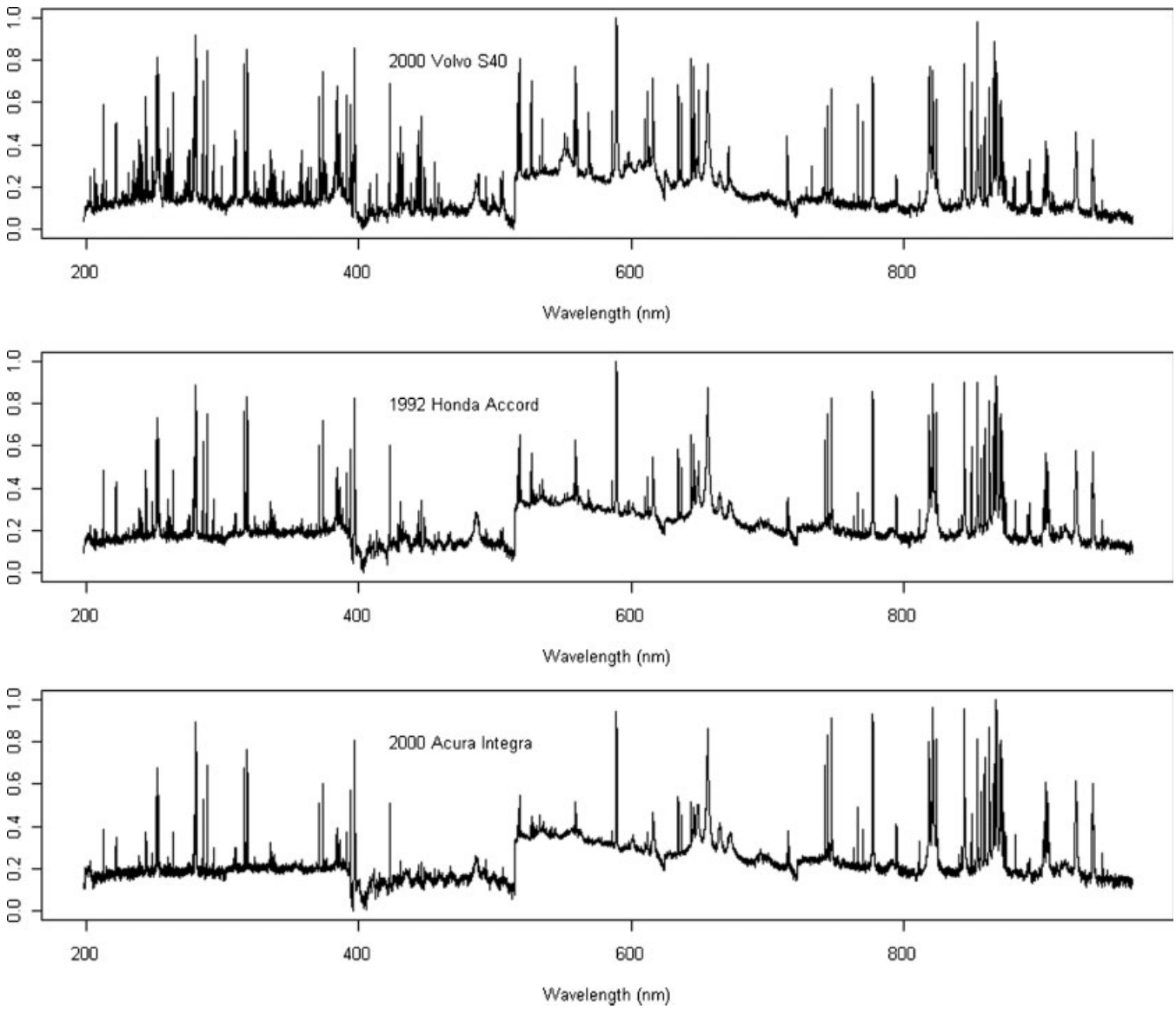


**Figure 1.** Representative LIBS spectral profiles from float glass samples taken from a 2000 Volvo S40, a 1992 Honda Accord and a 2000 Acura Integra. Spectral intensities are plotted on a log scale and normalized 0–1.

among the Honda spectra, (d) the 324 scores between the Honda and Acura, (e) the 153 similarity scores among the Acura spectra and (f) the 324 scores between the Volvo and the Acura. Figure 3 shows the box plots of these sets of similarity scores, which clearly demonstrates the potential for classification.

### 3.1. Measure of similarity

A popular choice, Pearson correlation coefficients, measures the strength of linear dependency between two spectra. It is invariant to linear transformations, which makes our analysis robust. Suppose we have two spectra denoted as $x = (x_1, x_2, ..., x_k)$and $y = (y_1, y_2, ..., y_k)$. Their correlation coefficient is defined as

$$r_{xy} = \frac{\sum_i (x_i - \bar{x})(y_i - \bar{y})}{\sqrt{\sum_i (x_i - \bar{x})^2}\sqrt{\sum_i (y_i - \bar{y})^2}} \quad (1)$$

If $(x_i, y_i)$, $i = 1, 2, ..., k$, are independently and identically distributed from a bivariate normal distribution, as $k$ increases the $r_{xy}$ approximately follows a normal distribution with the mean being the population correlation coefficient $\rho_{xy}$and the variance $(1 - \rho_{xy}^2)^2/(k - 1)$. However, when $\rho_{xy}$ is near 1 (which would be the case when we consider two spectra from the same composition), the normal approximation does not work well. As a remedy, a transformation of $r_{xy}$ suggested by Fisher [25],

$$f_{xy} = 0.5 \ln[(1 + r_{xy})/(1 - r_{xy})] \quad (2)$$

usually achieves better normal approximation with mean $0.5 \ln[(1 + \rho_{xy})/(1 - \rho_{xy})] + 0.5\rho_{xy}/(k - 1)$ and variance $1/(k - 3)$. However, since the subscripts $i = 1, 2, ..., k$ indicate the wavelengths, $(x_i, y_i)$ are anticipated to have different means, thus they are not identically distributed. The independence of adjacent measurements could also be problematic. Therefore, the normality of Pearson correlation or its transformation is not automatically guaranteed.



  

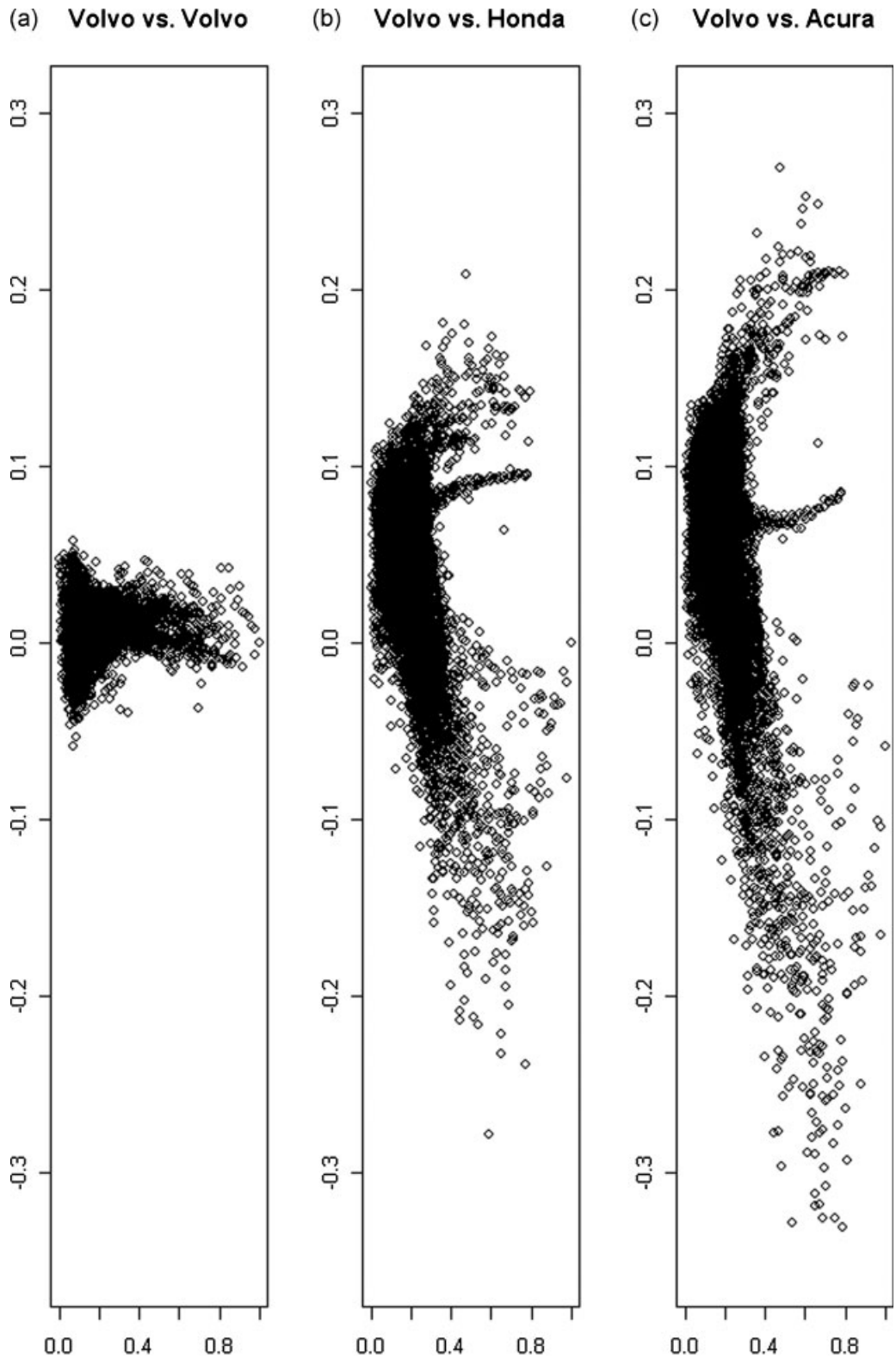


**Figure 2.** Scatter plots of the spectral intensities of the 2000 Volvo shown in Figure 1, against (a) another 2000 Volvo spectrum, (b) against a 1992 Honda spectrum and (c) against a 2000 Acura spectrum.

We consider the 153 pairwise Pearson correlation coefficients calculated between 18 spectra from the 1992 Honda, where $k = 13\,696$ wavelengths is quite large. Both the Pearson correlation and its Fisher transformation are clearly skewed as shown in Figure 4, which is inconsistent with an assumption of normality. Later we develop a non-parametric test, where the test statistic, a weighted average of $f_{xy}$, exhibits even stronger evidence against the normality.

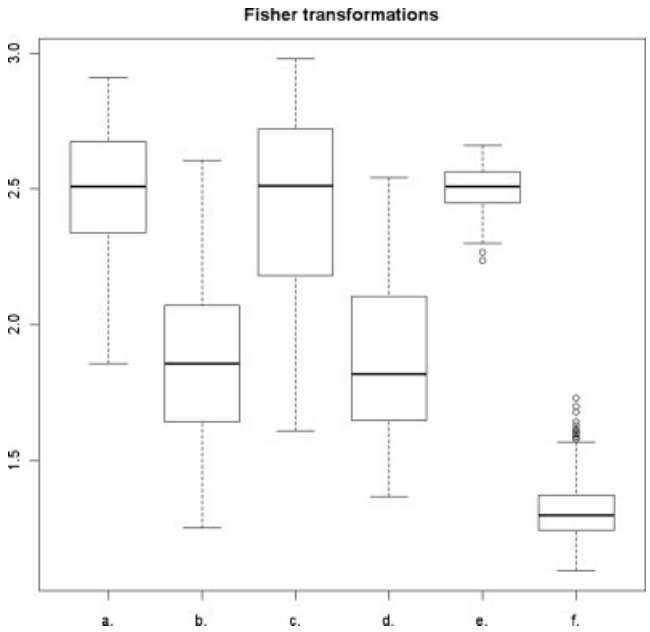


**Figure 3.** Box-plots of the similarity scores resulting from Fisher transformations of the Pearson correlations between (a) 2000 Volvo spectra, (b) 2000 Volvo and 1992 Honda spectra, (c) 1992 Honda spectra, (d) 1992 Honda and 2000 Acura spectra, (e) 2000 Acura spectra and (f) 2000 Acura and 2000 Volvo spectra.

Fortunately, the information about the distribution of $r_{xy}$ or $f_{xy}$ is not crucial if we have multiple spectra from the same sample. We can study the relative magnitude of between-sample $f_{xy}$ and within-sample $f_{xy}$ to make sound decisions without specific information about their distributions, which leads to a non-parametric permutation test [16].

### 3.2. Permutation test

For ease of exposition, we first introduce some notation. Let $\{X_1, X_2, \ldots, X_m\}$ and $\{X_{m+1}, X_{m+2}, \ldots, X_{m+n}\}$ represent two sets of spectra ($m$ spectra in set 1 and $n$ spectra in set 2) taken from two samples respectively, where each vector $X_i$ is an independent realization of the corresponding elemental composition. Define $S_1 = \{1, 2, \ldots, m\}$ and $S_2 = \{m+1, m+2, \ldots, m+n\}$ as two index sets. Let $f_{ij}$ be a similarity function between $X_i$ and $X_j$. While in this study we use the Fisher transformation defined in Equation (2), in principle, all the results in this paper are valid for any reasonable measurement of similarity.

We define the summation of similarities within a set of spectra ($T_1$ and $T_2$) and between two sets of spectra ($T_3$), as shown in Equations (3)–(5).

$$T_1 = \sum_{(i,j)\in S_1, i\neq j} f_{ij} \tag{3}$$

$$T_2 = \sum_{(i,j)\in S_2, i\neq j} f_{ij} \tag{4}$$

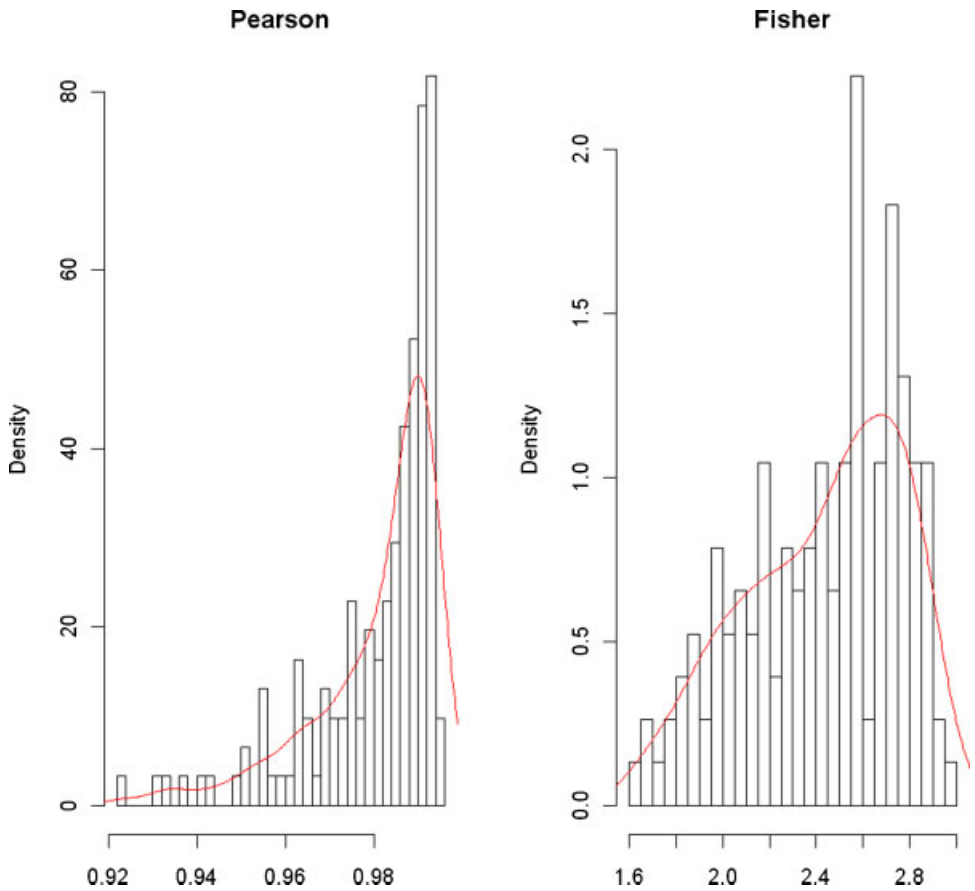


**Figure 4.** Distribution of Pearson correlations and the Fisher transformations from 153 pairwise comparisons between 18 LIBS spectra from a 1992 Honda glass sample. Each spectrum contained wavelengths. Both the Pearson correlation and its Fisher transformation are clearly skewed.



  

$$T_3 = \sum_{i \in S_1, j \in S_2} f_{ij} \tag{5}$$

The test statistic, $W$, is then defined as shown in Equation (6):

$$W = \frac{T_1 + T_2}{m(m-1) + n(n-1)} - \frac{T_3}{mn} \tag{6}$$

When the null hypothesis is true, the expected value of $W$ equals zero, since the within-sample and between-sample similarity measures will follow the same distribution. When the alternative hypothesis is true, i.e. the two samples have different profiles resulting from differing elemental compositions, we expect the within-sample similarity measures are higher than the between-samples measures. Consequently, $W$ tends to be larger. Without a reliable knowledge of the distribution of $f_{ij}$, assuming specific parametric models for $W$ can be misleading. We adopt a non-parametric permutation test for this study, although results from a Wald test, which assumes a normal distribution for $W$ will be presented for comparison. Under the non-parametric permutation test, for a total of $m+n$ spectra, there will be ${}_{m+n}C_m = (m+n)!/(m!n!)$ different combinations (i.e. different ways to choose $m$ out of $m+n$ unique objects) which will lead to ${}_{m+n}C_m$ values of $W$. These values follow the same distribution under the null; no assumption is necessary with regard to the normality or other form of the distribution of $r_{ij}$, $f_{ij}$ or $W$.

Minimizing both Type I and Type II errors are of interest for hypothesis testing. In Type I errors, it is concluded that two spectral profiles are different, when in fact they are the same. In the case examined here, all samples are known to come from different vehicles. We assume these profiles should be different unless additional information indicates otherwise. Thus a Type II error occurs when we conclude that two samples' profiles match and therefore the samples may have been the same, when in fact the samples were different. A large value of $W$ supports the alternate hypothesis. Therefore, the $p$-value of the test is the proportion of the ${}_{m+n}C_m$ values that are greater than or equal to the observed $W$. For example, in the experiments reported here (six spectra per sample) there are ${}_{12}C_6 = 924$ combinations. Suppose that for one test, the observed $W$ is ranked 879th among these 924 values; thus the $p$-value would be $(924 - 878)/924 = 0.0498$. A rejection region $\{W \geq c\}$ defines a desirable balance between the Type I error ($\alpha$) and Type II error ($\beta$), as defined in expressions (7) and (8):

$$\alpha = \Pr\{\text{reject } H_0 | H_0\} = \Pr\{W \geq c | H_0\} \tag{7}$$

$$\beta = \Pr\{\text{accept } H_0 | H_A\} = \Pr\{W < c | H_A\} \tag{8}$$

It is well known that for parametric tests, any deviation from the assumed distribution may shift the actual size of the Type I error from the nominal $\alpha$ level. In contrast, the actual $\alpha$ level of the permutation test automatically holds because when the null is true, all $W$ values are exchangeable having the identical distribution. Suppose that $c$ is set to be the 95th percentile of all $W$ values from the permutations, the significance level is automatically set at $\alpha = 0.05$. Of course, the value of $\beta$ depends on the magnitude of the difference between different samples (different glasses in this case), which manifests itself in the distribution of $W$.

### 3.3. Wald test

To test the mean of a generic test statistic equals zero, the Wald test is a widely used technique, which compares the ratio of a test statistic and its (estimated) standard deviation, $z = W/\text{sd}(W)$, to a standard normal distribution. However, the validity of this test hinges on the proximity of the distribution of $W$ to normality. Even though the non-parameteric test does not require normality, it can be informative to compare the permutation test with its Wald test counterpart. Under the null hypothesis, we have $E(W) = 0$. If we let $E[f_{ij}] = \mu$, $\text{var}(f_{ij}) = \sigma^2$, $\text{cov}(f_{ij}, f_{kl}) = 0$ and $\text{cov}(f_{ij}, f_{jk}) = \delta$, then

$$\text{var}(W) = \left(\frac{2}{m(m-1) + n(n-1)} + \frac{1}{mn}\right)\sigma^2 + \left(\frac{-4mn(m+n-2)}{[m(m-1) + n(n-1)]^2} + \frac{m+n-2}{mn}\right)\delta \tag{12}$$

Estimates for the means and variances can be written as

$$\hat{\mu}_1 = \sum f_{ij}/[m(m-1)], \quad \text{where } (i,j) \in S_1$$

$$\hat{\sigma}^2 = \left[\sum_{(i,j) \in S_1} (f_{ij} - \hat{\mu}_1)^2 + \sum_{(i,j) \in S_2} (f_{ij} - \hat{\mu}_2)^2\right] / [m(m-1) + n(n-1)]$$

$$\hat{\delta} = \frac{\sum_{(i,j,k) \in S_1} (f_{ij} - \hat{\mu}_1)(f_{ik} - \hat{\mu}_1) + \sum_{(i,j,k) \in S_2} (f_{ij} - \hat{\mu}_2)(f_{ik} - \hat{\mu}_2)}{m(m-1)(m-2) + n(n-1)(n-2)}$$

where $i$, $j$ and $k$ are all different. With these estimates for the mean, variance and covariance, we obtain a plug-in estimate of $\text{var}(W)$.

To study the distribution of the Wald test statistic, we revisited the 18 spectra from the 1992 Honda. Without replacement, we randomly selected two sets, each with six spectra. Permutation test statistic, its non-parametric $p$-value and its Wald test $p$-value were calculated, respectively. We repeat this procedure 500 times. Figure 5a shows the histogram of these 500 values of $W$. Figure 5b shows the quantile–quantile plot of non-parametric $p$-values against a standard uniform distribution, which shows an excellent match between normal $\alpha$ levels and actual levels. In contrast, the quantile–quantile plot of Wald test $p$-value against a standard uniform distribution shown in Figure 5c indicates a huge departure. The skewness of $W$ in Figure 5a also confirms our earlier skepticism of the normality of $f_{ij}$. If $f_{ij}$ is approximately normal, $W$ should be even closer to normal since it is a linear combination of $f_{ij}$s, which is clearly not the case.

### 3.4. Power of the test

We first investigate the initial set of three vehicles. For any pair of samples, we randomly select six spectra out of 18 for each sample and apply the permutation test on them. We repeat this procedure 500 times. The largest $p$-value for comparing Volvo vs. Honda is 0.0022; those for Volvo vs. Honda and Honda vs. Acura are 0.0022 and 0.0043, respectively. At significance level set at 1%, we will discriminate between these three vehicles 100% of the time. While the Wald test's theoretical foundation is incorrect in this case, we examine its performance as well. The maximum Wald $p$-value from all these tests is less than $10^{-5}$.

Next we apply both the permutation test and the Wald test on the sets of LIBS spectra from 10 automobile float glass samples

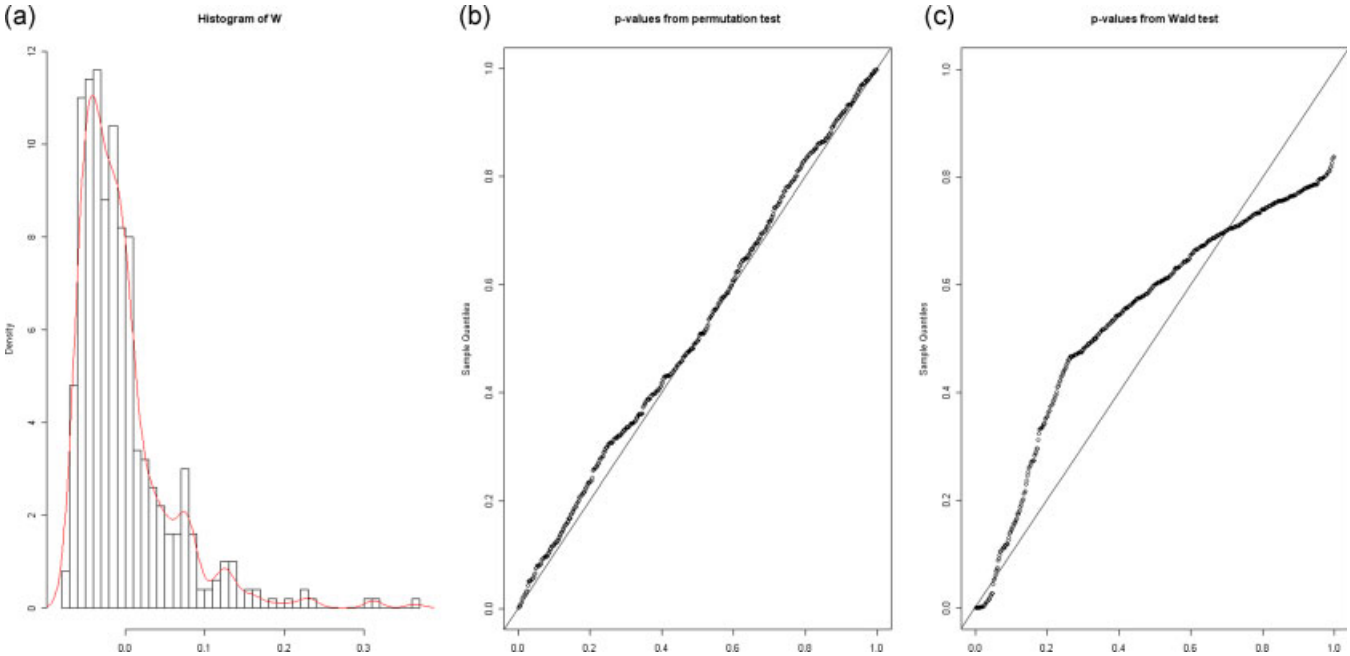


**Figure 5.** Results from non-parametric and Wald tests for *W* calculated for 500 sets of randomly selected spectra (two sets comprised of six spectra each), chosen without replacement from 18 spectra from the 1992 Honda glass. (a) The histogram of the 500 W values. (b) The quantile–quantile plot of non-parametric *p*-values against a standard uniform distribution. (c) The quantile–quantile plot of Wald test *p*-value against a standard uniform distribution.

**Table I.** Manufacturer and make of automobiles that were the source for the glass samples used in this study

| Year | Manufacturer | Make |
|---|---|---|
| 1978 | GMC | Van |
| 1979 | Volkswagon | Rabbit |
| 1989 | Dynasty | Dynasty |
| 1992 | Honda | Accord |
| 1993 | Mazda | 626 |
| 1997 | Chrysler | Sebring |
| 1998 | Mitsubishi | Galant |
| 1998 | Mitsubishi | Galant |
| 2000 | Volvo | S40 |
| 2000 | Acura | Integra |

from 10 different vehicles, including two 1998 Mitsubishi Galant automobiles. These 10 vehicles are listed in Table I. For each vehicle, a dataset containing six spectra was collected from the center part of the window. There are 45 pairwise comparisons between the different automotive glass samples. The maximum *p*-value from the permutation test is 0.0087. Again we have 100% differentiation if the significance level is set at 1%. Note that the two Mitsubishi Galant glass samples were also differentiated. The maximum Wald *p*-value is also less than $10^{-5}$. The Wald test has demonstrated high differentiation capability in past studies as in this study, which has made it less likely to detect its invalidity.

## 4. DISCUSSION

The non-parametric test performs well for the glass samples examined in this study. Deviation of the transformed correlation coefficients from normality may lead to an artificially high or low size of Type I error for the Wald test. With the non-parametric approach, the size of the Type I error is guaranteed set at the prescribed significance level. Meanwhile, the permutation test has demonstrated excellent capability of differentiating different profiles, even when they seem highly similar.

The non-parametric permutation approach can also be readily applied to other type of data, e.g. UV–visible absorption, FTIR, Raman and fluorescence spectra, etc. In this study, the log transformation of the glass spectral intensities served to de-emphasize the most intense peaks which is similar in spirit to the idea of masking peaks but avoids the complication of identifying masking areas [11]. While there is no significant difference between working on original scale or on log scale for this study, we recommend the permutation test on the log transformed spectra for the glass samples.

## Acknowledgements

This work was supported under Award number 2006-DN-BX-K251 from the Office of Justice Programs, National Institute of Justice, Department of Justice. Points of view in this document are those of the authors and do not necessarily represent the official position of the U.S. Department of Justice. Ni's research was supported in part by Grant DMS-0805409 from National Science Foundation. The work was done at the National Center for Forensic Science, the University of Central Florida.

## REFERENCES

1. Lee Y-I, Sneddon J. Recent developments in instrumentation for laser induced breakdown spectroscopy. *ISIJ Int.* 2002; **42**: S129.
2. Lee W, Wu J, Lee Y, Sneddon J. Recent applications of laser-induced breakdown spectrometry: a review of material approaches. *Appl. Spectrosc. Rev.* 2004; **39**: 27.



  

3. Hahn DW, Miziolek AW, Palleschi V. Laser-induced breakdown spectroscopy: an introduction to the feature issue. *Appl. Opt.* 2003; **42**: 5937.
4. Rusak DA, Castle BC, Smith BW, Winefordner JD. Recent trends and the future of laser-induced plasma spectroscopy. *Trend Anal. Chem.* 1998; **17**: 453.
5. Kuzuya M, Murakami M, Maruyama N. Quantitative analysis of ceramics by laser-induced breakdown spectroscopy. *Spectrochim. Acta B* 2003; **58**: 957.
6. Bridge CM, Powell J, Steele KL, Sigman ME. Forensic comparative glass analysis by laser-induced breakdown spectroscopy. *Spectrochim. Acta B.* 2007; **62**: 1419.
7. Copley GJ. The composition and manufacture of glass and its domestic and industrial applications. In *Forensic Examination of Glass and Paint*, Caddy B (ed.). Taylor & Francis: New York, NY, 2001; 27–46.
8. Brends-Montero S, Wiarda W, de Joode P, van der Pejil G. Forensic analysis of float glass using laser ablation inductively coupled plasma mass spectrometry (LA-ICP-MS): validation of a method. *J. Anal. At. Spectrom.* 2006; **21**: 1185.
9. Bridge CM, Powell J, Steele KL, Williams M, MacInnis JM, Sigman ME. Characerization of automobile float glass with laser-induced breakdown spectroscopy and laser ablation inductively coupled plasma mass spectrometry. *Appl. Spectrosc.* 2006; **60**: 1181.
10. Naes BE, Umpierrz S, Ryland S, Barnett C, Almirall JR. A comparison of laser ablation inductively coupled plasma mass spectrometry, micro X-ray fluorescence spectroscopy, and laser induced breakdown spectroscopy for the discrimination of automotive glass. *Spectrochim. Acta B* 2008; **63**: 1145.
11. Rodriguez-Celis EM, Gornushkin IB, Heitmann UM, Almirall JR, Smith BW, Winefordner JD, Omenetto N. Laser induced breakdown spectroscopy as a tool for discrimination of glass for forensic applications. *Anal. Bioanal. Chem.* 2008; **391**: 1961.
12. Curran JM, Triggs CM, Almirall JR, Buckleton JS, Walsh K. The interpretation of elemental composition measurements from forensic glass evidence: I. *Sci. Justice* 1997; **37**(4): 241–2244.
13. Curran JM, Triggs CM, Almirall JR, Buckleton JS, Walsh K. The interpretation of elemental composition measurements from forensic glass evidence: II. *Sci. Justice* 1997; **37**(4): 245–249.
14. Campbell GP, Curran JM. The interpretation of elemental composition measurements from forensic glass evidence III. 2009; **49**: 2–7.
15. Michel APM, Chave AD. Analysis of laser-induced breakdown spectroscopy spectra: The case for extreme value statistics. *Spectrochim. Acta B* 2007; **62**: 1370.
16. Good P. Permutation, Parametric and Bootstrap Tests of Hypotheses, 3rd edn. Springer-Verlag: New York, NY, 2004.
17. Zadora G. Classification of glass fragments based on Elemental composition and refractive index. *J. Forensic Sci.* 2009; **54**: 49.
18. Zadora G. Evaluation of evidence value of glass fragments by likelihood ratio and Bayesian network approaches. *Anal. Chim. Acta* 2009; **642**: 279.
19. Zadora G. Glass analysis for forensic purposes—a comparison of classification methods. *J. Chemom.* 2007; **21**: 174.
20. Lucy D. *Introduction to Statistics for Forensic Scientists*. JohnWiley & Sons: Chichester, 2005.
21. The R Foundation for Statistical Computing Version 2.9.0, http://www.r-project.org/
22. Feldmann M, Weismann R. Initial stages of float glass corrosion. *J. Non-Cryst. Solids* 1997; **218**: 205.
23. Smith NJ, Pantano CG. Leached layer formation on float glass surfaces in the presence of acid interleave coatings. *J. Am. Ceram. Soc.* 2008; **91**: 736.
24. Curran JM, Hicks TN, Buckleton JS. *Forensic Interpretation of Glass Evidence*. CRC Press: New York, NY, 2000; 17.
25. Fisher RA. *Statistical Methods for Research Workers*. Oliver & Boyd: Edinburgh, 1925 (14th ed. reprinted by Hafner Publishing Co., New York, 1973); 199–206.

  